Journal of Peptide Science
J. Pept. Sci. 2007; **13**: 413–421
Published online 8 May 2007 in Wiley InterScience (www.interscience.wiley.com). DOI: 10.1002/psc.865

JOURNAL OF PEPTIDE SCIENCE

Conformation–activity relationship of peptide T and new pseudocyclic hexapeptide analogs

ANNAMARIA D'URSI,[a] GIUSEPPE CALIENDO,[b] ELISA PERISSUTTI,[b] VINCENZO SANTAGADA,[b] BEATRICE SEVERINO,[b] STEFANIA ALBRIZIO,[a] GIUSEPPE BIFULCO,[a] SUSANNA SPISANI[c] and PIERO A. TEMUSSI[d,e]*

[a] Dipartimento di Scienze Farmaceutiche, Universita` di Salerno, 84084-Fisciano Italy
[b] Dipartimento di Chimica Farmaceutica e Tossicologica, Università di Napoli Federico II, 80131 Napoli, Italy
[c] Dipartimento di Biochimica e Biologia Molecolare, Università di Ferrara, 44100 Ferrara,Italy
[d] Dipartimento di Chimica, Università di Napoli Federico II, Complesso Universitario di Monte S. Angelo, 80126 Napoli, Italy
[e] National Institute for Medical Research, Medical Research Council, London NW7 1AA, UK

Received 1 February 2007; *Revised 20 March 2007*; *Accepted 22 March 2007*

Abstract: Peptide T (ASTTTNYT), a segment corresponding to residues 185–192 of gp120, the coat protein of HIV, has several important biological properties *in vitro* that have stimulated the search for simpler and possibly more active analogs. We have previously shown that pseudocyclic hexapeptide analogs containing the central residues of peptide T retain considerable chemotactic activity. We have now extended the design of this type of analogs to peptides containing different aromatic residues and/or Ser in lieu of Thr. The complex conformation-activity relationship of these analogs called for a reexamination of the basic conformational tendencies of peptide T itself. Here, we present an exhaustive NMR conformational study of peptide T in different media. Peptide T assumes a γ-turn in aqueous mixtures of ethylene glycol, a type-IV β-turn conformation in aqueous mixtures of DMF, and a type-II β-turn conformation in aqueous mixtures of DMSO. The preferred conformations for the analogs were derived from modeling, starting from the preferred conformations of peptide T. The best models derived from the γ-turn conformation of peptide T are those of peptides **XII** (DSNYSR), **XIII** (ETNYTK) and **XVI** (ESNYSR). The best models derived from the type-IV β-turn conformation of peptide T are those of peptides **XIV** (KTTNYE) and **XV** (DSSNYR). No low-energy models could be derived starting from the type-II β-turn conformation of peptide T. The analogs with the most favored conformations are also the most active in the chemotactic test.

Keywords: chemotaxis; conformation; NMR; peptide T; pseudocyclic analogs

INTRODUCTION

Peptide T (ASTTTNYT), the sequence of which corresponds to region 185–192 of the gp120 coat protein, was originally proposed as an inhibitor of the binding of HIV-1 to the CD4 receptor [1]. Although the original observations were not followed by successful clinical applications, it was later found that peptide T is endowed with several interesting biological activities [2,] notably with a potent chemotactic activity on human monocytes, which in turn is correlated with the inhibition of CD4 binding [3,4].

Invasion of cells by HIV-1 is a more complex phenomenon than believed at the time of the discovery of peptide T. It has been shown that in addition to the CD4 primary cell receptor the interaction of the gp120 envelope protein involves another cell surface molecule, a co-receptor, belonging to the chemokine receptor family [5]. The two main co-receptors indicated so far are CCR-5 and CXCR-4, instead of, or in conjunction with, CCR-5 [6].

The determination of the crystal state structure of a gp120–CD4-CD4i antibody complex [7] did not clarify the role of peptide T in the interaction. The CD4-induced antibody (CD4i) mimics in part the HIV-1 co-receptor but the recombinant gp120 utilized in the X-ray diffraction study was a 'core fragment' depleted of some variable regions including that in which peptide T is contained (variable region V2). Modeling of loop V1/V2 showed that it is located above the gp120 core, close to the interface with CD4i [7]. It is therefore conceivable to think that the region of gp120 that contains the sequence of peptide T is involved in an interaction with the co-receptor, in lieu of or in addition to that with the CD4 receptor.

The involvement of peptide T in an interaction with a chemokine receptor, implying a possible interpretation for its chemotactic activity, prompted us to resume SAR studies on this peptide and its analogs [8]. To favor pseudocyclization, we designed hexapeptides containing a core typical of peptide T (either the TNYT or the TTNY sequence) flanked by charged residues at the two ends. Peptides carrying an acidic residue

Abbreviations: Boc, *t*-butyloxycarbonyl; DIPCDI, *N*,*N*′-diisopropylcarbodiimide; DMF, dimethylformamide; DMSO, dimethylsulfoxide; EG, ethylene glycol; HOBt, *N*-hydroxybenzotriazole; N^{α}-Fmoc, N^{α}-(9-fluorenylmethoxycarbonyl); Pmc, 2,2,5,7,8-pentamethyl-chroman-6-sulfonyl; Trt, tripheylmethyl; PITC, phenylisothiocyanate; For, formyl; QM, quantum mechanical; TFA, trifluoro acetic acid.

*Correspondence to: P. A. Temussi, Dipartimento di Chimica, Università di Napoli Federico II, Complesso Universitario di Monte S. Angelo, 80126 Napoli, Italy; e-mail: temussi@unina.it

at the *N*-terminus and a basic residue at the *C*-terminus feature stable helical structures and retain full chemotactic activity. Owing to the importance of aromatic residues and to the widespread occurrence in sequence data bases of typical peptide T cores in which Thr is replaced by Ser, we have extended the design of pseudocyclic T peptides to hexapeptides containing Ser in lieu of Thr and Phe or Trp in lieu of Tyr. While most of these substitutions induced only small changes in the chemotactic activity, in three cases, apparently minor changes, such as Lys in lieu of Arg, induced large variations in biological activity (*vide infra*). In our view, these surprising results may be best interpreted on conformational grounds. However, an exploratory NMR work showed that all analogs exist as complex mixtures of conformations in equilibrium. Therefore, we resorted to modeling methods, based on canonical conformations of the parent peptide. As a necessary prerequisite for the conformational study of the analogs, a novel detailed study of peptide T was deemed necessary since, in spite of several published results of experimental and theoretical investigations, there is no consensus on the preferred conformation of this peptide [9].

MATERIALS AND METHODS

Solid-phase Synthesis of Peptides

Peptides were numbered following the eight hexapeptide series of the previous paper [8]. The first two, **I**, D-TNYT-R, and **II**, E-TNYT-R, coincide in fact with the corresponding ones of this reference. The other peptides are: **IX**, DTNFTR; **X**, DSNFSR; **XI**, DTNWTR; **XII**, DSNYSR; **XIII**, ETNYTK; **XIV**, KTTNYE; **XV**, DSSNYR; and **XVI**, ESNYSR. All peptides, including peptide T, were prepared by solid-phase methods, using a continuous-flow instrument employing an on-line UV monitoring system (Milligen/Biosearch, Ventura, CA, USA, model 9050). The stepwise syntheses were carried out by Fmoc chemistry, without any special effort to optimize the repetitive steps. For each peptide, 0.5 g (0.35 mequiv.) of Wang resin (Novabiochem, Laufelfingen, Switzerland) was used. The resin was swelled in DMF for 1 h and packed in the reaction column. *tert*-Butyl was used as the side-chain protecting group for Ser, Thr, Asp, Tyr, and Glu. Boc was used for Lys and Trp, while Pmc and Trt were used for Arg and Asn, respectively. N^{α}-Fmoc amino acids were used in fourfold excess with, as coupling reagents, DIPCDI in the presence of HOBt for 1 h. The Fmoc group was removed with a flow of 20% piperidine in DMF for 25 min. After completion of the synthesis, each protected peptide was cleaved from the resin, and the amino acid side chains were simultaneously deprotected by treatment with a mixture of TFA/H_2O/Et_3SiH (88 : 5 : 7) for 2 h (4 h in case of Arg-containing peptides) at room temperature. The resin was removed by filtration and washed with TFA (2 × 1 ml). The filtrate and washings were combined and evaporated at 25 °C, and the oily residue was triturated with diethyl ether (10 ml). The resulting solid peptide was collected by centrifugation and purified by preparative RP-HPLC (purification yield, 75–85%). Verification of the chemical structures was achieved by amino acid analysis, mass spectrometry, and NMR spectroscopy.

Homogeneity and retention times of the purified products were assessed by analytical RP-HPLC with a Vydac C_{18} column (5 μm, 4.6 × 250 mm, spherical) connected to a Rheodyne model 7725 injector, a Waters 600 HPLC system, a Waters 486 tunable absorbance detector set to 220 nm, and a Waters 746 chart recorder. Analytical determinations were carried out with the following gradient system: A, 0.1% TFA in CH_3CN; B, 0.1% TFA in H_2O; linear gradient from 0% A–100% B to 30% A–70% B over 30 min, flow rate 1 ml/min. The final HPLC purity of the peptides was always greater than 99%.

Preparative RP-HPLC was routinely performed on a Waters Delta-Prep 4000 system equipped with a Waters 486 multiwavelength detector, using a Vydac C_{18} (15–20 μm, 20 × 250 mm) column. The gradient used was the same as that for the analytical determinations. The flow rate was 30 ml/min.

Solvents used for reactions were dried over 3 Å molecular sieves. DMF was distilled immediately before use over CaH_2. All solvents were filtered and degassed prior to use. Reagent grade materials were purchased from Novabiochem and from Sigma-Aldrich (Milan, Italy), and were used without further purification. Amino acid analyses were carried out using the PITC methodology (Pico-Tag, Waters-Millipore, Waltham, MA). Lyophilized samples of peptides (50–100 pmol) were placed in heat-treated borosilicate tubes (50 × 4 mm), sealed, and hydrolyzed using 200 μl of 6 N HCl containing 1% phenol in the Pico-Tag work station for 1 h at 150 °C. A Hypersil ODS column (250 × 4.6 mm, 5 μm particle size) was employed to separate the PITC-amino acid derivatives.

Molecular weights of peptides were determined by fast atom bombardment-mass spectrometry (FAB/MS) on a ZAB 2 SE-Fisons (Beverly, MA, USA) instrument.

Analytical data of the new peptides synthesized are summarized in Table 1.

Monocyte Chemotaxis

Mononuclear cells were isolated from heparinized blood of normal human volunteers by sedimentation over Ficoll-Paque (Pharmacia, Uppsala, Sweden). Chemotaxis was performed in a modified 48-multiwell Boyden chamber (Neuroprobe, Inc., Milano, Italy). The migration into the filter was evaluated by the method of leading front [10] as previously described [11]. Each compound was dissolved in DMSO at a concentration of 10^{-2} M, diluted before use with Krebs–Ringer phosphate buffer containing 0.5 mg/ml bovine serum albumin (Sigma-Aldrich, St Louis, MO, USA), and tested at a final concentration in the range 10^{-13} M to 10^{-5} M. To obtain an accurate comparison, the results for the individual compounds are expressed in terms of chemotactic index (CI), which is the ratio: (migration towards test attractant – migration towards the buffer)/migration towards the buffer. Migration in presence of the buffer alone was 35 μm ± 3 SE ($n = 8$). In all experiments, 10^{-8} M fMLP (For-Met-Leu-Phe-OH) was used as a peptide control; peak response migration was 67 μm ± 3 SE (CI 0.92 ± 0.03).

NMR

Samples for NMR spectroscopy were prepared by dissolving each peptide in water, adjusting the pH to a value between

DOI: 10.1002/psc

Table 1 Analytical data of new pseudocyclic peptide T analogs

Peptide		Amino acid analysis										HPLC[a]	MW	
		D	**T**	**N**[b]	**F**	**R**	**S**	**W**[b]	**Y**	**E**	**K**		Calcd	Found
IX	**DTNFTR**	1.81	1.96	—	1.01	0.96	—	—	—	—	—	16.1	752.8	753.6
X	**DSNFSR**	1.90	—	—	0.95	0.94	1.94	—	—	—	—	16.3	724.7	725.6
XI	**DTNWTR**	1.85	1.90	—	—	1.04	—	—	—	—	—	16.9	791.8	792.3
XII	**DSNYSR**	1.82	—	—	—	0.96	1.91	—	0.89	—	—	15.6	740.7	741.4
XIII	**ETNYTK**	0.86	1.87	—	—	—	—	—	0.91	1.03	1.01	15.4	754.8	755.1
XIV	**KTTNYE**	0.88	2.01	—	—	—	—	—	0.94	0.97	1.02	15.5	754.8	755.4
XV	**DSSNYR**	1.84	—	—	—	1.01	1.98	—	0.99	—	—	15.6	740.7	741.6
XVI	**ESNYSR**	0.85	—	—	—	0.96	1.89	—	1.01	1.01	—	15.9	754.8	755.7

[a] Retention time for the following conditions: reversed phase Vydac C_{18} column (5 μm, 4.6 × 250 mm) and the following gradient system: A, 0.1% TFA in CH_3CN; B, 0.1% TFA in H_2O; linear gradient from 0% A–100% B to 30% A–70% B over 30 min, UV detection at 220 nm, flow rate 1 ml/min.
[b] The method used for hydrolysis does not allow the recovery of tryptophan, while asparagine is completely converted to aspartic acid.

6 and 7 by addition of small amounts of 1 M NaOH, and lyophilization of aliquots corresponding to a concentration of 1.0 mM in 0.5 ml of solvent. The composition of the cryomixtures water/DMSO, water/DMF, and water/EG was 20/80 v/v in all cases. Redissolution in media different from neat water was achieved by addition of *ca* 500 μl of the appropriate solvent.

NMR spectra were recorded on Bruker (Karlsruhe, Germany) DRX-400 and DRX-600 spectrometers. One-dimensional NMR spectra were acquired in the temperature range 295–330 K in the Fourier mode with quadrature detection, and the water signal was suppressed by a low-power selective irradiation in the homogated mode. Assignments of ^{1}H resonances were achieved by a combination of standard 2D experiments: DQF-COSY [12,] TOCSY [13,] and NOESY [14]. All experiments were run in the phase-sensitive mode using quadrature detection in ω_1 by time-proportional phase incrementation of the initial pulse [15]. Data block sizes were 2048 addresses in t_2 and 350 equidistant t_1 values. Before Fourier transformation, the time domain data matrices were multiplied by shifted cosine functions in both dimensions. A mixing time of 70 ms was used for the TOCSY experiments. NOESY experiments were run at 300 K with mixing times in the range 100–250 ms. The qualitative and quantitative analyses of DQF-COSY, TOCSY, and NOESY spectra were achieved using the SPARKY [16] and the NMRView [17] software.

Structure Calculations

Peak lists were converted into the format used by DYANA 1.5 [18] and translated into upper distance bounds with the routine CALIBA; the necessary pseudoatom corrections were applied for nonstereospecifically assigned protons at prochiral centers and for the methyl group of Thr. After discarding redundant and duplicated constraints, the final list included 36 intraresidue and 20 interresidue constraints for the structure of peptide T in EG/water, 47 intraresidue and 18 interresidue constraints for the structure of peptide T in DMSO/water, and 29 intraresidue and 12 interresidue constraints for the structure of peptide T in DMF/water. These restraints were used to generate an ensemble of 50 structures by the standard protocol of simulated annealing in torsion angle space implemented in DYANA (using 6000 steps). No dihedral angle restraints or hydrogen-bond restraints were applied. The best 20 structures, which had low values of the target functions (0.83–1.19), were refined by *in vacuo* minimization in the AMBER 1991 force field, using the program SANDER of the AMBER 5.0 suite [19].

To mimic the effect of solvent screening, all net charges were reduced to 20% of their real value, and moreover a distance-dependent dielectric constant ($\varepsilon = r$) was used. The cutoff for nonbonded interactions was 12 Å. The NMR-derived upper bounds were imposed as semiparabolic penalty functions, with force constants of 16 kcal/mol Å^2; the function was shifted to linear when the violation exceeded 0.5 Å. The best ten structures after minimization had AMBER energies ranging from −441.4 to −391.1 kcal/mol. The final structures were analyzed using the Insight 98.0 program. Computations were performed on SGI Indigo II computers.

Model Building

Model building of the analogs was performed by means of the program Chem3D (Cambridge Soft, Cambridge, MA, USA). Starting models were built from scratch using only sequence information and imposing local conformations consistent with those previously found for peptide T (this work). The resulting conformer was energy-minimized using a simple MM2 force field *in vacuo* with a dielectric constant of 15, and NOE-derived interatomic distances as the only restraints. Restrained minimization was continued until low values of the gradient (<0.001) were reached.

Quantum Mechanical Calculations

The initial geometries of the minimum-energy conformers obtained from the NMR-restrained molecular dynamics, in which the terminal –OH was substituted with an $-OCH_3$ group, were preliminarily optimized with the ONIOM method [20,21,] which allowed the application of different levels of

DOI: 10.1002/psc

theory to different parts of peptide T. In particular, we combined the B3LYP functional and the 6–31G(d) basis set for the ^{3}TTT^{5} segment and the AM1 semiempirical method for the remaining residues. Subsequently, on the obtained geometry, a final full optimization was run on the whole molecule at the hybrid DFT B3LYP level using the 6–31G(d) basis set (Gaussian03 software package) [22].

RESULTS

Chemotactic Activity

The biological activity of the hexapeptides **IX–XVI** was assessed by measuring their ability to stimulate monocyte-directed migration (chemotaxis). Table 2 summarizes the results for all new pseudocyclic analogs (shown in bold), including the parent peptides (HEXA-I, HEXA-II, HEXA-III, and HEXA-VIII) described in Ref. 8 for the sake of comparison.

For all new analogs, Figure 1 shows the migration of monocytes in response to concentration gradients ranging from 10^{-13} to 10^{-5} M. While all analogs have a substantial chemotactic activity, the changes introduced by substituting the single aromatic residue (Y with F or W), or both T with S and at the two terminals (E/D and R/K), modulate the activity. The peptides can be grouped into two families (shown in Figure 1A and 1B, respectively), mainly on the basis of their CI and substitutions. The most dramatic effect can be seen in peptides with different aromatic residues; both peptides **IX** and **X**, hosting F in lieu of Y, have rather low potency. On the contrary, substitution of T with S leads to a modest decrease in potency for **XII** with respect to I and to a considerable increase in the case of **XVI** *vs* II. The substitution S/T proved effective also in the case of peptide III, which is changed into the slightly more potent and effective peptide **XV**. The most dramatic increase in chemotactic activity is brought about by the mere change of *N*-terminal R of peptide VIII into K of its homologous peptide **XIV**. Modulations induced by the E/D and R/K substitutions, as in the previous series [8,] are not easy to interpret since the charges are conserved. Overall, it is fair to say that peptides **XII, XIV, XV,** and **XVI** have very high values both in activity and potency. The complexity of the conformation–activity relationship precludes a simplistic analysis based solely on chemical constitution and calls for a detailed conformational analysis.

Table 2 Biological activity of all pseudocyclic analogs, expressed as molar concentration of the peptide at the maximum of the chemotactic index (CI)

Peptide	Sequence	M_{max} (CI)
HEXA -I	DTNYTR	−11 (0.67)
HEXA-IX	**DTNFTR**	**−11 (0.41)**
HEXA-X	**DSNFSR**	**−10 (0.51)**
HEXA-XI	**DTNWTR**	**−8 (0.62)**
HEXA-XII	**DSNYSR**	**−11 (0.59)**
HEXA-II	ETNYTR	−11 (0.68)
HEXA-XVI	**ESNYSR**	**−10 (0.93)**
HEXA-XIII	**ETNYTK**	**−8 (0.87)**
HEXA-III	DTTNYR	−11 (0.68)
HEXA-XV	**DSSNYR**	**−11 (0.79)**
HEXA-VIII	RTTNYE	−8 (0.55)
HEXA-XIV	**KTTNYE**	**−10 (0.82)**

Structure of Peptide T

A whole set of 1D and 2D proton spectra of peptide T were recorded in three aqueous mixtures: DMF/water 80/20 v:v, DMSO/water 80/20 v:v, and EG/water 80/20 v:v. To check the absence of aggregation, several spectra were acquired in the concentration range 0.5–15 mM. No significant changes were observed in the distribution and shape of the ^{1}H resonances,

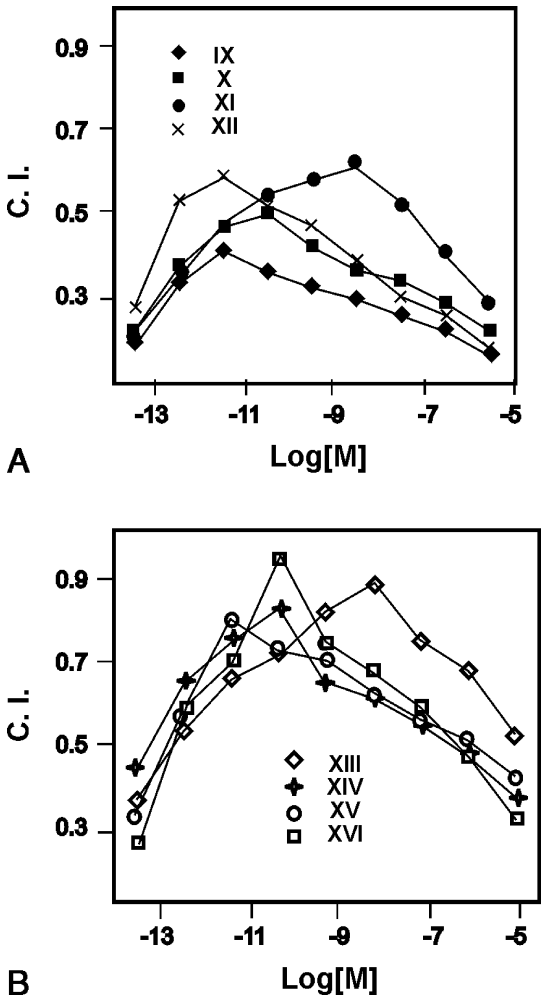

Figure 1 Migration of human monocytes in response to concentration gradients, ranging from 10^{-13} to 10^{-5} M. The experimental points of the chemotactic index (CI) are the mean of five separate experiments. SEs are within 10% of the mean value. (A) Peptides **IX –XII**; (B) Peptides **XIII–XVI**.

DOI: 10.1002/psc

Table 3 Chemical shifts of peptide T in DMSO/H_2O 80:20 v/v; DMF/H_2O 80:20 v/v, and EG/H_2O (600 MHz, temperature 300K)

Residues	Solvents	NH	CHα	Hβ2	Hγ2	Hδ	Hε
	DMSO/H_2O	8.06	3.84	1.31			
Ala1	DMF/H_2O		4.11	1.48	2.17		
	EG/H_2O		3.95	1.40	2.11		
	DMSO/H_2O	8.57	4.43	3.57/3.65			
Ser2	DMF/H_2O	8.03	4.50	3.77			
	EG/H_2O	8.06	4.49	3.78			
	DMSO/H_2O	7.79	4.27	4.03	1.01		
Thr3	DMF/H_2O	8.04	4.39	4.02	1.2		
	EG/H_2O	7.98	4.33	4.19	1.08		
	DMSO/H_2O	7.74	4.28	3.99	0.99		
Thr4	DMF/H_2O	8.01	4.37	4.22	1.07		
	EG/H_2O	7.98	4.31	4.12	1.05		
	DMSO/H_2O	7.69	4.21	3.95	0.97		
Thr5	DMF/H_2O	7.82	4.31	4.15	1.02		
	EG/H_2O	7.87	4.21	4.00	0.97		
Asn6	DMSO/H_2O	8.00	4.49	2.32/2.48	6.90/7.36		
	EG/H_2O	8.13	4.57	2.54/2.62	7.47/6.79		
	DMSO/H_2O	7.85	4.43	2.65/2.91		6.59	7.00
Tyr7	DMF/H_2O	8.14	4.45	2.80/3.02		6.65	7.02
	EG/H_2O	7.98	4.47	2.81/3.02		6.96	6.67
	DMSO/H_2O	7.86	4.09	4.12	1.02		
Thr8	DMF/H_2O	7.59	4.46	4.08	1.00		
	EG/H_2O	7.47	4.03	4.06	1.00		

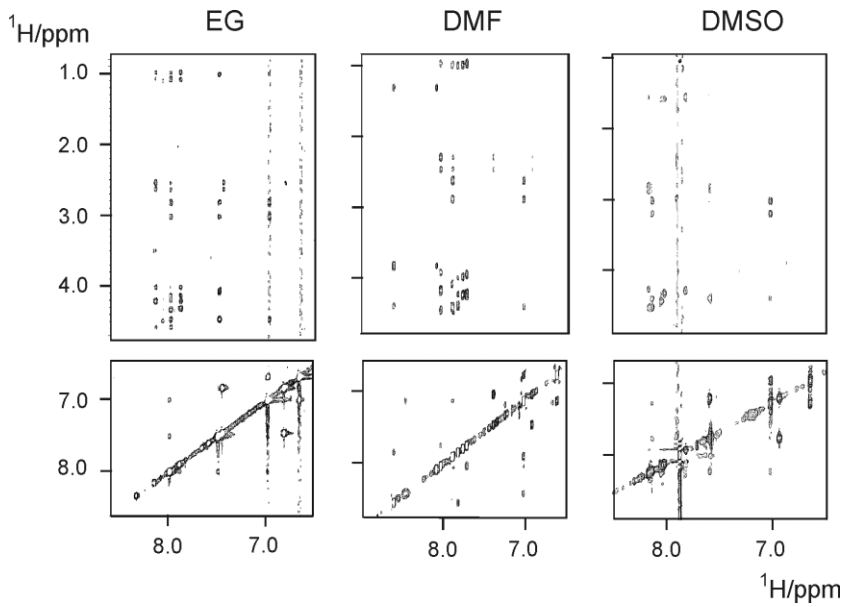

Figure 2 Partial NOESY spectra of peptide T in three aqueous mixtures: EG/water 80/20 v:v (left), DMF/water 80/20 v:v (center) and DMSO/water 80/20 v:v (right).

indicating that no aggregation phenomena occurred in this concentration range.

Sequential resonance assignments of the proton spectra of peptide T in the three different mixtures (Table 3) were made by the approach described by Wüthrich [23].

Despite the small size of the peptide, the inspection of the NOESY spectra evidences the presence of a significant number of NOE effects (Figure 2). The pattern of NOEs correlation is consistent with the preference of the peptide to assume ordered, folded conformations in the *C*-terminal region.

DOI: 10.1002/psc

Detailed structure calculations by means of the DYANA software were based on the NOE interprotonic distances, as restraints were derived from the spectra in the three aqueous mixtures. The structures of peptide T calculated on the basis of NOE data are fully consistent with the qualitative evaluation of the NOESY spectra.

Figure 3 shows (on the left panel) a neon representation of the models corresponding to the three conformations generated by MOLMOL [24] and the corresponding solvent accessible surfaces generated by Chem3D (on the right panel). The pdb file corresponding to the EG/water solution, subjected to PROMOTIF software [25] for the validation of the structural results, shows the presence of a γ-turn [26] involving residues ^{5}TNY^{7} (Figure 3A). The angles characterizing this turn are 73.8 and −59.2 for ϕ_4 and ψ_4, respectively. Unconstrained minimization of the structures did not produce in this region any major rearrangement, which would instead be expected if the observed dihedrals were imposed by the influence of artifactual NMR restraints.

The above procedure, repeated for the data in DMF/water and DMSO/water, generated NMR conformations that can be classified as β-turns at the *C*-terminus [27]. The angles that characterize the conformations are (ϕ_4, −116; ψ_4, 7.7; ϕ_5, −175.9; ψ_5, 3.3) and (ϕ_4, −50.2; ψ_4, 90.5; ϕ_5, 64.7; ψ_5, 9.1) for DMF/water and DMSO/water respectively. The analysis of the pdb files using the PROMOTIF software yields

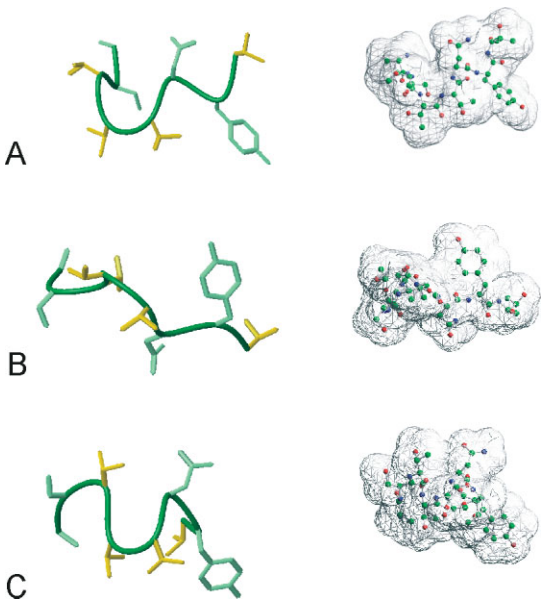

Figure 3 Comparison of the models of peptide T corresponding to the three solvent systems with the corresponding solvent accessible surfaces. The neon models were generated by MOLMOL [24]: the side chains of the neon representations are colored in pale green but for Thr residues (gold). The corresponding solvent accessible surfaces were generated by Chem3D (on the right panel). (A) Conformation in EG/water 80/20 v : v; (B) Conformation in DMF/water 80/20 v : v; (C) Conformation in DMSO/water 80/20 v : v.

a type-IV β-turn [28] involving residues 3–6 (^{3}TTTN^{6}) for the peptide T in DMF/water (Figure 3B) and a type-II β-turn involving the same residues in DMSO/water (Figure 3C).

A type-II β-turn of course is unexpected for residues of L-chirality. In fact, both results are rather unusual and, in the case of the type-IV turn, the experimental values of the torsion angles are not very close to the ideal expected values [25]. Although many papers use the classification 'type-IV' for any turn not otherwise classified, a statistical survey of many proteins by Hutchinson and Thornton [29] does give the most likely values: −61, 10, −53, 17 for $\phi(i+1)$, $\psi(i+1)$, $\phi(i+2)$ and $\psi(i+2)$, respectively. Our experimental values are not very close to these, particularly $\phi(i+1)$ and $\phi(i+2)$, which are closer to those of the extended conformations. However, as such they they are even farther away from allowing intramolecular stabilizing hydrogen bonds. It is likely that these conformations are the result of specific interactions of the Thr side chains with the mixed solution media. A comparison of the calculated models of peptide T in DMSO/water, DMF/water, and EG/water shows a common tendency to fold in a turn conformation in the central/*C*-terminal portion of the sequence. An inspection of the side chains highlights a common orientation of the Thr residues, in which the hydroxyl moieties seem to play a critical role for the contact with the receptor.

Nonetheless, we took both the experimental torsion angles and the canonical ones suggested by PROMOTIF as a useful basis for further calculations, both for peptide T and for its pseudocyclic analogs.

Quantum Mechanical Optimization of the Peptide T Geometry

The somewhat low number of NMR restraints used in the structure calculation of peptide T does not allow a very detailed structural description. To obtain additional information on conformational details, a QM optimization of the energy and geometry of the molecule was performed using the hybrid DFT functional and the 6–31 G(d) basis set (see Materials and methods). The NMR DMSO/H_2O solution structure was chosen as the initial geometry for the DFT optimization, since in this solvent system the model was generated using the highest number of constraints. The geometry obtained from the QM calculations is still fully consistent with the NMR experimental restraints, but it shows a number of interactions that were not observed in the previously obtained NMR structures. In particular, a type-II β-turn at Thr^{4}-Thr^{5} (Table 4) is suggested from the presence of hydrogen bonds between the T^{3} CO group and the N^{6} NH group, and between T^{4} CO and Y^{7} NH. Such folding of the peptide backbone seems to be further stabilized by the hydrogen bond involving the hydroxyl moiety of T^{3} and the CO function

DOI: 10.1002/psc

of T [8]. Finally, the side chains of ^{2}TT^{3}, interacting via a hydrogen bond through their hydroxyl moieties, provide a structural motif which may be representative of peptides containing adjacent Thr residues.

Models of Analogs

All analogs of peptide T reported in this work (**IX–XVI**) are too short to yield a sufficient number of NOE-derived constraints to perform a full structure determination. For all analogs, instead of recurring to the standard structure determination employed for the parent peptide, we built models that were subsequently refined by restrained energy minimization. In order to build good starting conformations, we adopted ϕ angles close to those of the three basic structures found for peptide T, with small manual adjustments to take into account experimental distance restraints. The sequences of all peptides are consistent with the γ–turn centered on the N residue, whereas only peptides **XIV** and **XV** can adopt conformations consistent with type-IV and type-II turns, simply because of their sequences flanked by the charged *N*-terminal residues.

Each peptide was energy-minimized using a simple MM2 force field *in vacuo* and using NOE-derived interatomic distances as the only restraints. After several cycles of restraint minimization, unrestrained energy minimization led to a final conformation that was checked for consistency *vs* the NMR spectra.

In terms of energy, the best models derived from the γ–turn conformation of peptide T are those of peptides **XII, XVI,** and **XIII**, with a difference of *ca* 10 kcal/mol with respect to the next model (**XI**). The molecular models are shown in Figure 4.

The best model derived from the type-IV β-turn conformation of peptide T is that of peptide **XIV**, but that of peptide **XV** is of comparable energy. On the contrary, for models derived from the type-II β-turn conformation of peptide T, those of peptides **XIV** and **XV** are very high in energy with respect to those of previous models.

Table 4 Φ and Ψ dihedral angles (^{3}TTTNA^{6} segment) of the peptide T backbone as derived from QM calculations

Residue	Φ	Ψ
Thr3	−61.81	10.70
Thr4	−55.72	141.77
Thr5	60.21	28.19
Asn6	68.19	21.55
Ala7	−83.50	80.16

DISCUSSION

Several conformations have been proposed in the literature for peptide T [8,9,30–36]. The first conformational study was performed by NMR spectroscopy in a DMSO solution [30]. On the basis of diagnostically relevant chemical shifts, NOE, and variable temperature data, the authors hinted that peptide T adopts an unusual degree of conformational order. The data are consistent with a β-turn including the four *C*-terminal residues (TNYT). Soon afterwards, the same authors refined the conformational analysis and extended it to the *C*-terminal pentapeptide fragment (TTNYT) [31,32]. This pentapeptide segment, although less structured, showed some tendency to fold even in a conformation similar to that of the parent peptide. According to Cotelle *et al.* [33], the conformation of the synthetic pentapeptide TTNYT is at variance with the conclusion of Motta *et al.* [31] since their NMR data allow the proposal for two distinct β-turn arrangements. However, their peptide has all the side chains fully protected and

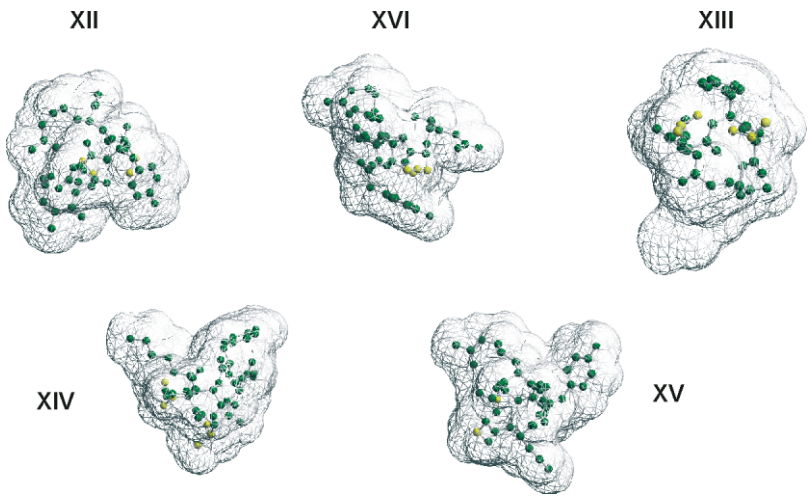

Figure 4 Best models for analogs **XII, XIII** and **XVI** consistent with a γ–turn centered on the N residue, and for analogs **XIV** and **XV** consistent with the type-IV and type-II β-turns, respectively.

DOI: 10.1002/psc

N- and *C*-terminal groups blocked by *t*-butoxycarbonyl and benzyloxy groups, respectively. A fully protected peptide does not have, in general, the same biological properties of the parent peptide, nor can it easily assume the same conformation when protection of the labile protons involves many of its residues.

While peptide T forms a β-turn in DMSO, Zangger and Sterk [34] found no evidence for such a structure in water when the conformation of peptide T in aqueous solution was investigated by means of NMR spectroscopy. Peptide T exists in aqueous medium in a random coil conformation with an increased tendency to form a partly populated β-strand at the ends of the peptide backbone. This finding is not too surprising since very few linear peptides can adopt ordered structures in water.

Andrianov and Akhrem [35], on the basis of restrained molecular dynamics calculations, reinterpreted the above NMR data to propose six different conformations for peptide T and suggested that the carbonyl oxygen of Thr4 might be involved in a bifurcated hydrogen bond with amide protons of Tyr7 and Thr8.

The complexity of the conformational tendencies of peptide T, emerging from all previous studies, is best illustrated by the theoretical investigation of Filizola *et al.* [36].

In order to define the conformational preferences for peptide T, these authors undertook a thorough exploration of the conformational space within the framework of the molecular mechanics, using simulated annealing as a searching strategy. The results of the search indicated that the peptide exhibits an α-helical character, although most of the conformations characterized can be described as bent conformations. The analysis of the low-energy conformations revealed a high tendency of the peptide to adopt bent structures, some of which exhibit a helical character. Some of the structures characterized, albeit less populated than other conformations, exhibit also β-turns.

Overall, the results of the present thorough conformational search support previous experimental findings of a β-turn conformation as one of the accessible structures of the peptide, but do not support the hypothesis that this is the most populated conformation. The experimental conformational analysis of peptide T presented here, based on a 'solvent scan' approach, not only clarifies the issue of the conformational preferences of peptide T but also provides firm bases to analyze the pesudocyclic analogs.

Among the three conformations found in the present work, only that found in DMF bears some similarity with the most favored conformations predicted by Filizola *et al.* [36,] precisely with their conformation number VIII. This finding confirms that peptide T can indeed be regarded as a chameleon peptide. In the light of our NMR investigation, it is clear that rather than trying to define *the* most stable conformation or *the* bioactive conformation, it is necessary to acknowledge that its conformation is more dependent on the precise environment than that of any other bioactive peptide.

This behavior may be linked, at least in part, to the high content of Thr or Ser residues, the side chains of which may favor ordered solvation. The possible role of these residues is suggested not only by the common orientation of their hydroxyl moieties in peptide T itself but also by the similar orientation of the same moieties in the pseudocyclic analogs.

Acknowledgements

This work was supported by grants from Regione Campania (Legge 41. Annualità 1998) and funds from the University of Ferrara (ex 60%) and from MIUR (FIRB 2003). We wish to thank Prof. D. Picone and Dr R. Spadaccini for the collection of NMR spectra of the cyclic analogs and Banca del Sangue of Ferrara for providing fresh blood.

REFERENCES

1. Pert CB, Hill JM, Ruff MR, Berman RM, Robey WG, Arthur LO, Ruscetti FW, Farrar WL. Octapeptides deduced from the neuropeptide receptor-like pattern of antigen T4 in brain potently inhibit the human immunodeficiency virus receptor binding and T-cell infectivity. *Proc. Natl. Acad. Sci. U.S.A.* 1986; **83**: 9254–9258.
2. Brenneman DE, Buzy JM, Ruff MR, Pert CB. Peptide T sequences prevent neuronal cell death produced by the envelope protein (gp120) of the human immunodeficiency virus. *Drug Develop. Res.* 1988; **15**: 361–369.
3. Ruff MR, Martin BM, Ginns EI, Farrar WL, Pert CB. CD4 receptor binding peptides that block HIV infectivity cause human monocyte chemotaxis. *FEBS. Lett.* 1987; **211**: 17–22.
4. Marastoni M, Salvadori S, Balboni G, Scaranari V, Spisani S, Reali E, Traniello S, Tomatis R. Structure-activity relationships of a cyclic and linear peptide T analogues. *Int. J. Pept. Protein Res.* 1993; **41**: 447–454.
5. Baggiolini M. Chemokines and leukocyte traffic. *Nature* 1998; **392**: 565–568.
6. Cairns JS, D'Souza MP. Chemokines and HIV-1 second receptors: the theraupetic connection. *Nat. Med.* 1998; **4**: 563–568.
7. Kwong PD, Wyatt R, Robinson J, Sweet RW, Sodroski J, Hendrickson WA. Structure of an HIV gp120 envelope glycoprotein in complex with the CD4 receptor and a neutralizing human antibody. *Nature* 1998; **393**: 648–659.
8. Picone D, Rivieccio A, Crescenzi O, Caliendo G, Santagada V, Perissutti E, Spisani S, Traniello S, Temussi PA. Peptide T revisited: conformational mimicry of epitopes of anti-HIV proteins. *J. Pept. Sci.* 2001; **7**: 197–207.
9. De Dios AC, Sears DN, Tycko R. NMR Studies of peptide T, an inhibitor of HIV infectivity, in an aqueous environment. *J. Pept. Sci.* 2004; **10**: 622–630.
10. Zigmond SH, Hirsch JG. Leukocyte locomotion and chemotaxis: new method for evaluation and demonstration of a cell derived chemotactic factor. *J. Exp. Med.* 1973; **137**: 387–395.
11. Bisaccia F, Castiglione-Morelli MA, Spisani S, Ostuni A, Serafini-Fracassini A, Bavoso A, Tamburro AM. The amino acid sequence coded by the rarely expressed exon 26A of human elastin contains a stable turn with chemotactic activity for monocytes. *Biochemistry* 1998; **37**: 11128–11135.

12. Piantini U, Soerensen OW, Ernst RR. Multiple quantum filters for elucidating NMR coupling networks. *J. Am. Chem. Soc.* 1982; **104**: 6800–6801.
13. Bax A, Davis DG. MLEV-17-based two-dimensional homonuclear magnetization transfer spectroscopy. *J. Magn. Reson.* 1985; **65**: 335–360.
14. Jeener J, Meyer BH, Bachman P, Ernst RR. Investigation of exchange processes by two dimensional NMR spectroscopy. *J. Chem. Phys.* 1979; **71**: 4546–4553.
15. Marion D, Wüthrich K. Application of phase sensitive two-dimensional correlated spectroscopy (COSY) for measurements of ^1H–^1H spin-spin coupling constants in proteins. *Biophys. Res. Commun.* 1983; **113**: 967–971.
16. Goddard TD, Kneller DG. *SPARKY 3*, University of California: San Francisco, 2006.
17. Johnson BA, Blevins RA. NMRView: a computer program for the visualization and analysis of NMR data. *J. Biomol. NMR* 1994; **4**: 603–614.
18. Güntert P, Mumenthaler C, Wüthrich K. Torsion angle dynamics for NMR structure calculation with the new program DYANA. *J. Mol. Biol.* 1997; **273**: 283–298.
19. Pearlman DA, Case DA, Caldwell JW, Ross WS, Cheatham TE III, DeBolt S, Ferguson D, Seibel G, Kollman PA. AMBER, a package of computer programs for applying molecular mechanics, normal mode analysis, molecular dynamics and free energy calculations to simulate the structural and energetic properties of molecules. *Comput. Phys. Commun.* 1995; **91**: 1–41.
20. Svensson M, Humbel S, Froese RDJ, Matsubara T, Sieber S, Morokuma K. ONIOM: a multilayered integrated MO + MM method for geometry optimizations and single point energy predictions. A test for Diels-Alder reactions and $Pt(P(t\text{-}Bu)_3)_2 + H_2$ oxidative addition. *J. Phys. Chem.* 1996; **100**: 19357–19363.
21. Dapprich S, Komaromi I, Byun KS, Morokuma K, Frisch MJ. A new ONIOM implementation in Gaussian 98. Part I. The calculation of energies, gradients, vibrational frequencies and electric field derivatives. *J. Mol. Struct.* 1999; **1**: 461–462.
22. Frisch MJ, Trucks GW, Schlegel HB, Scuseria GE, Robb MA, Cheeseman JR, Montgomery Jr JA, Vreven T, Kudin KN, Burant JC, Millam JM, Iyengar SS, Tomasi J, Barone V, Mennucci B, Cossi M, Scalmani G, Rega N, Petersson GA, Nakatsuji H, Hada M, Ehara M, Toyota K, Fukuda R, Hasegawa J, Ishida M, Nakajima T, Honda Y, Kitao O, Nakai H, Klene M, Li X, Knox JE, Hratchian HP, Cross JB, Bakken V, Adamo C, Jaramillo J, Gomperts R, Stratmann RE, Yazyev O, Austin AJ, Cammi R, Pomelli C, Ochterski JW, Ayala PY, Morokuma K, Voth GA, Salvador P, Dannenberg JJ, Zakrzewski VG, Dapprich S, Daniels AD, Strain MC, Farkas O, Malick DK, Rabuck AD, Raghavachari K, Foresman JB, Ortiz JV, Cui Q, Baboul AG, Clifford S, Cioslowski J, Stefanov BB, Liu G, Liashenko A, Piskorz P, Komaromi I, Martin RL, Fox DJ, Keith T, Al-Laham MA, Peng CY, Nanayakkara A, Challacombe M, Gill PMW, Johnson B, Chen W, Wong MW, Gonzalez C, Pople JA. *Gaussian 03, Revision B.05*. Gaussian: Wallingford, 2004.
23. Wüthrich K. *NMR of Proteins and Nucleic Acids*. John Wiley & sons: New York, 1986.
24. Koradi R, Billeter M, Wüthrich K. MOLMOL: a program for display and analysis of macromolecular structure. *J. Mol. Graphics* 1996; **14**: 51–55.
25. Hutchinson EG, Thornton JM. PROMOTIF-a program to identify and analyze structural motifs in proteins. *Protein Sci.* 1996; **5**: 212–220.
26. Nemethy G, Printz MP. The γ turn, a possible folded conformation of the polypeptide chain. comparison with the β turn. *Macromolecules* 1972; **5**: 755–758.
27. Venkatachalam CM. Stereochemical criteria for polypeptides and proteins. V. Conformation of a system of three linked peptide units. *Biopolymers* 1968; **6**: 1425–1436.
28. Lewis PN, Momany FA, Scheraga HA. Chain reversals in proteins. *Biochim. Biophys. Acta* 1973; **303**: 211–229.
29. Hutchinson EG, Thornton JM. A revised set of potentials for β-turn formation in proteins. *Protein Sci.* 1994; **3**: 2207–2216.
30. Picone D, Temussi PA, Marastoni M, Tomatis R, Motta A. A 500 MHz study of peptide T in DMSO solution. *Febs. Lett.* 1988; **231**: 159–163.
31. Motta A, Picone D, Temussi PA, Marastoni M, Tomatis R. Conformational analysis of peptide T and its C-pentapeptide fragment. *Biopolymers* 1989; **28**: 479–486.
32. Temussi PA, Picone D, Castiglione-Morelli MA, Motta A, Tancredi T. Bioactive conformation of linear peptides in solution: an elusive goal? *Biopolymers* 1989; **28**: 91–107.
33. Cotelle N, Lohez M, Cotelle P, Henichart JP. Conformational study of the threonine-rich C-terminal pentapeptide of peptide T. *Biochem. Biophys. Res. Commun.* 1990; **171**: 596–602.
34. Zangger K, Sterk H. Conformation of peptide T in aqueous solution. Determination of homonuclear coupling constants by selective HOHAHA techniques. *Magn. Reson. Chem.* 1995; **33**: 421–425.
35. Andrianov AM, Akhrem AA. Model of peptide T three-dimensional structure. *Mol. Biol.* 1993; **27**: 576–582.
36. Filizola M, Centeno NB, Perez JJ. Computational study of the conformational domains of peptide T. *J. Pept. Sci.* 1997; **3**: 85–92.

DOI: 10.1002/psc